

Model for Characterizing Photovoltaic Arrays with Shaded Solar Cells

C. A. Melo, *MS Student, IST*, J. M. Ferreira de Jesus, *Member, IEEE*

Abstract— This paper aims to study the basic principles and the importance of the development of a model for characterizing photovoltaic arrays with shaded cells. It will also include the future methodology of work and schedule, the motivation and definition of the problem under study. Photovoltaic energy is one of the fastest growing renewable energies in recent years. However, its production is strongly affected by the shading (total and partial) of the modules responsible for its production. This shading causes a mismatch between the cells, reducing the global production of the panel. It's necessary to know the effects of shading in the production of energy, for different configuration of photovoltaic modules, in order to understand which is less affected and why. For this, a model for characterizing photovoltaic arrays is created, whose equivalent circuit parameters change depending on the operation conditions (irradiance and temperature). Through an analysis based on each cell that constitutes the module in study, this computational model is able to analyze photovoltaic modules in an efficient and effective way.

Keyword— Equivalent Circuit Parameters, Mismatch, Photovoltaic arrays, Shading, Solar Cells

I. INTRODUCTION

The increasing consumption of electricity and the effects of global warming which have been becoming more noticeable led to an increased investment on renewable energy technologies, particularly photovoltaic (PV) energy. PV energy consists on the production of electric energy from the light that reaches the earth coming from the sun (photons), using photovoltaic models or arrays. [1]

However, the output power of a PV module or array decreases considerably due to many factors, being one of them shading or any other means that can cause non-uniform irradiation or temperature through the array. [2]

Before trying to eliminate or reduce this effect, it is necessary to better understand its origin, behavior and the effect it has on the solar cells of a module. Given that the field tests are expensive, time consuming and highly dependent on the weather conditions, it is of great importance to develop a reliable computational model that allows these tests to be

carried out quickly and accurately, under any conditions of operation.

The use of an equivalent circuit is a very convenient and common way to describe the electrical performance of electronic devices. These provide a number of advantages as being easy to understand and analyze, allows the devices' properties to be described in a simplified form and provides information related to complex physical processes that occur within the device. [3]

The equivalent circuit used to model the solar cells was the one diode and five parameters model, shown in Fig. 1. This model requires the five parameters to be known. All of them depend on the irradiance and temperature of the cell. [2]

The method used in this study to calculate the parameters considers this dependency. The values obtained are then used to train an artificial neural network (ANN), which will then be able to calculate the circuit parameters requiring only the irradiance and temperature of the cell, with minimal computational time.

After obtaining an ANN with a good enough accuracy, we begin the study for different operating conditions of PV arrays, based on the values of the parameters for each cell and including bypass diodes. All modules incorporate bypass diodes which are very important to protect the cells from overheating (hotspot) and non-recoverable reverse bias breakdown. [4]

The bypass diodes drastically change the module's I-V curve and several maximum power points (MPP) can be found in the P-V power-voltage curve of a module or array. Therefore, before analyzing partially shaded PV arrays, bypass diodes must be included in the model of the PV module.

The performance of the PV array depends on the shadow's size and shape. For this reason, it is crucial that the analyses of the PV array are made on a cell basis. However, the simulation of large-scale PV arrays requires a long computation time, which is why normally several series connected cells are considered as a single cell, thereby simplifying the computation.

The main aim of this study is to present a solar cell-based analyses method capable of simulating the effects of shading on a PV array, without increasing computational time and guarantying a good degree of precision. It is very difficult to simulate for all the possible shading scenarios. Besides, there are very different configurations possible for the PV arrays, so it is important to test all the operating conditions for all the

possible configurations because some of them may be better than others under some conditions and not in others.

So, in this study, various values of irradiance are used to study the behavior of different formations of PV arrays. To do so, there are used algorithms that evaluate the shading effects in PV arrays, which will be described together with some of the results obtained.

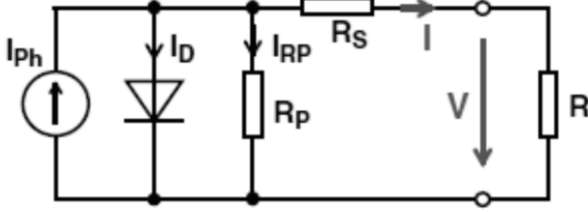


Figure 1 – Equivalent circuit of a solar cell.

II. DEVELOPMENT OF THE MODEL

The one diode and five parameters equivalent circuit consists on a diode, a current source and series and parallel resistances. The current source represents the photo-current I_{ph} generated when the cell is exposed to light. [2] The series resistance R_s represents the material losses and the semiconductor contact resistance, and R_p describes the leakage current resulting from parasitic currents between the top and bottom of the cell and inside the material due to impurities. [3]

For this model, the expression for the I-V curve is:

$$I = I_{ph} - I_s \left(e^{\frac{e(V-R_s I)}{n k T}} - 1 \right) - \frac{V - R_s I}{R_p} \quad (1)$$

Where I is the output current, I_s the diode's saturation current, q the electric charge ($1.6 \times 10^{-19} \text{C}$), V the terminal voltage of the module, n the ideality factor of the diode ($1 < n < 2$), k the Boltzman constant ($1.38 \times 10^{-23} \text{J/K}$), T the cell temperature (in K) and N_s the number of solar cells in series for a module. [2]

A. Determination of the parameters

To determine the parameters for the whole range of operating conditions, it is necessary to obtain points of the I-V curve (at least five points). To do so, it is used Sandia's PV Module Electrical Performance Model [5] to calculate the five points shown in figure 2.

Of the five required points, three of them are the ones usually used in the analysis of an I-V curve, that is the short-circuit current point $(0, I_{sc})$, the open-circuit voltage point $(V_{oc}, 0)$, and the maximum power point (V_{MP}, I_{MP}) . The other two, I_x and I_{xx} correspond to the current on the points:

$$V_x = 0.5 \times V_{oc} \quad (2)$$

$$V_{xx} = \frac{V_{MP} + V_{oc}}{2} \quad (3)$$

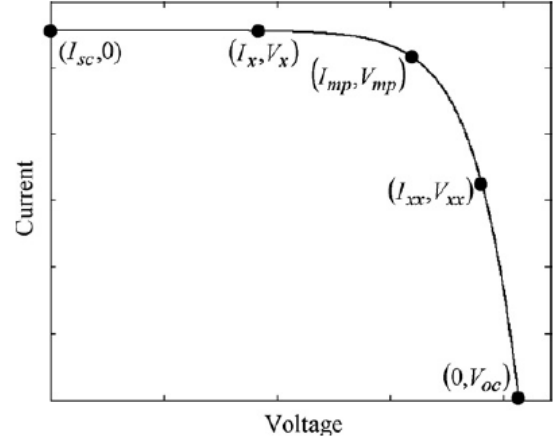


Figure 2 - The five operating points required to obtain the parameters for a given operating condition.

These points are calculated for temperatures between 15°C and 65°C , and irradiances between 100W/m^2 and 1000W/m^2 , on a Siemens SM 55 PV module. This module consists of 36 series connected monocrystalline silicon solar cells. Further specifications of the module are shown in Table 1.

Table 1 – Specifications of the Siemens SM 55 PV module.

(AM 1.5, 1000W/m^2 , 25°C)	
Maximum power P_{MP}	55W
Open circuit voltage V_{OC}	21.7V
Short circuit current I_{SC}	3.45A
Operating voltage at maximum power V_{MP}	17.4V
Operating current at maximum power I_{MP}	3.15A

After obtaining the five points of the curve, the Two-Step Linear Least-Squares Method (TSLLS) [6] is used to calculate the five parameters of the module.

B. Artificial Neural Network

Given the amount of operating conditions being studied, the TSLLS method is not a very efficient solution in terms of computing time and practicality. For this reason, all parameters are estimated using an ANN (Artificial Neural Network).

An ANN [7] is a technology that offers an alternative way to solve complex problems. In the last decade, significant progress has been made to expand the applicability of ANNs in several areas. If properly trained, the ANN can predict the equivalent circuit parameters by reading only the irradiance and temperature values.

It is used a three-layer neural network (see Fig. 3), and it was concluded that the most accurate result was obtained with 20 nodes. Thus, the input layer has 2 nodes (irradiance and temperature), the hidden layer has 20 and the output layer 5 nodes (I_{ph} , I_s , n , R_s and R_p).

Table 2 - Parameters of the equivalent circuit for different operating conditions.

Temperature (°C)	25	25	25	25	40	40	40	40	
Irradiance (W/m ²)	1000	800	600	400	1000	800	600	400	
Values using the TLSS	I_{ph} (A)	3,4567	2,7646	2,073	1,3817	3,4792	2,7826	2,0864	1,3906
	I_s (nA)	8,4047	3,7595	1,1554	0,22601	190,95	97,643	36,935	9,9276
	n	1,1845	1,1366	1,0716	0,99	1,268	1,2182	1,1507	1,067
	R_s (Ω)	0,4176	0,4383	0,4826	0,5867	0,3486	0,3501	0,3641	0,4104
	R_p (Ω)	216,582	260,392	332,898	475,734	203,873	244,790	312,401	445,282
Values using ANN	I_{ph} (A)	3,269	2,838	2,068	1,436	3,477	2,933	2,222	1,483
	I_s (nA)	8,297	4,352	0,4042	0,0415	181,4	97,49	36,12	10,91
	n	1,171	1,141	1,098	1,054	1,231	1,2	1,175	1,162
	R_s (Ω)	0,3058	0,4065	0,5023	0,6244	0,318	0,4314	0,431	0,3907
	R_p (Ω)	216,5	260,0	333,9	474,4	204,1	244,2	312,2	444,7

The attenuation function chosen for the hidden layer was the sigmoid function of hyperbolic tangent, and for the output layer a linear function.

ANN training requires a set of input/output target values $\{E(t), S(t)\}$. These include several output target values $S(t) = \{R_s(t), R_p(t), I_{ph}(t), I_s(t) \text{ and } n(t)\}$ corresponding to several input values $E(t) = \{T(t), G(t)\}$. The temperature values were defined between 10°C and 65°C and the irradiance between 100 W/m² and 1000W/m². Since the hidden layer activation function is a hyperbolic tangent function, all target values $\{E(t), S(t)\}$ are normalized between $[-1, 1]$. [8]

The training is performed by updating the weights and biases using an inverse propagation algorithm with the Levenberg-Marquardt optimization method to reduce the difference between target and output values, for data input values. This algorithm was chosen because it is considered to be the most appropriate for applications in problems involving non-linear equations, being this the case. [9] In Fig. 4 it is represented the mean squared error evolution during the training of the ANN.

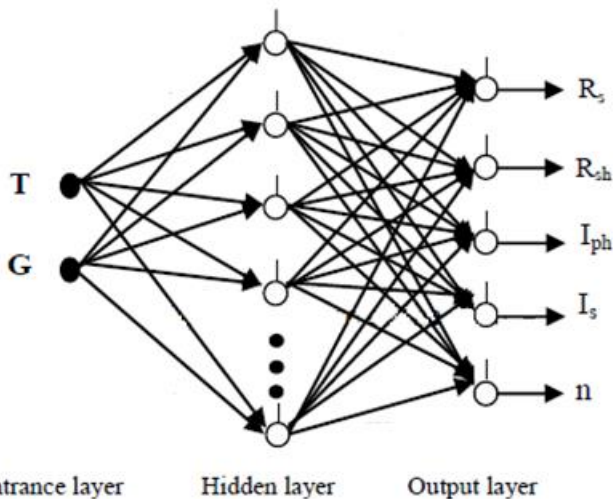


Figure 3 - Structure of the neural network to be used, with 2 input nodes, 20 nodes in the hidden layer and 5 output nodes.

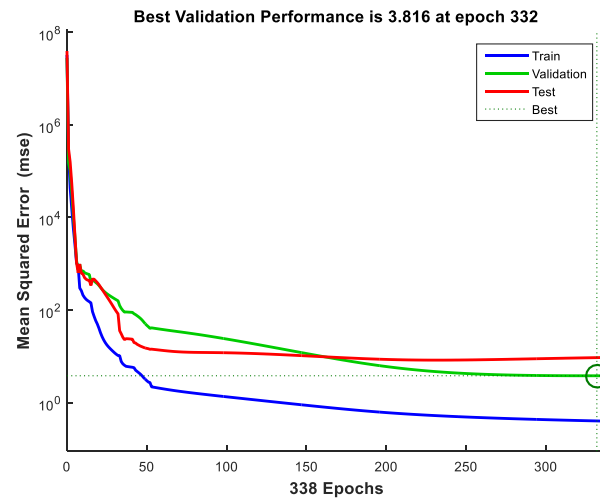


Figure 4 - Training, validation and test error after ANN training.

The results obtained at the output of the ANN are presented in Table 2, along with the values obtained using the TSLLS method. The values obtained for the parameters agree with other models that predict the variation of the parameters with the irradiance and the temperature. [10][11][12][13][14]

III. SIMULATION OF THE PHOTOVOLTAIC MODEL BASED ON A SOLAR CELL

When part of a photovoltaic module is shaded, cells that are shaded cannot produce the same current as unshaded cells. This leads to a series of situations that culminate in a state in which the shaded cells begin to dissipate power in the form of heat, this process is called hotspot.

To prevent these situations, bypass diodes are placed in the photovoltaic module. The presence of these diodes drastically changes the module's I-V curve, and several local maximum power points (MPP) can be formed in the P-V power-voltage curve of a module or system. This causes serious problems in

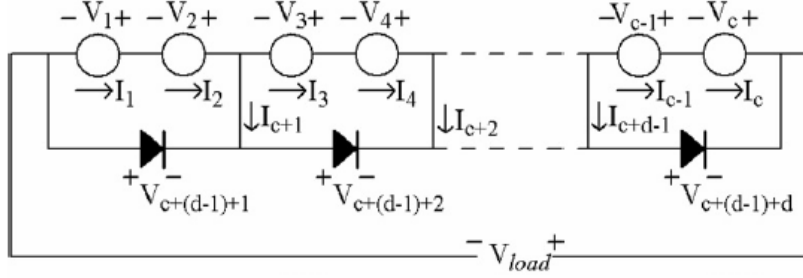


Figure 5- Illustrative model of a PV module in which the bypass diodes are connected to two solar cells.

the MPP control of the system. For this reason, before an analysis of partially shaded photovoltaic systems is carried out, the bypass diodes should be included in the model of the photovoltaic module.

The I-V characteristic curve depends on how the modules are shaded. The relationship between the MPP of a module, the number of cells shaded, and its level of irradiance will be defined through a cell-level analysis algorithm. The expressions that compose the algorithm are obtained using the laws of Kirchhoff for a given voltage V_{load} to the output of the module. [15]

A. Solar Cell Based Method

Considering c the total number of cells of the photovoltaic module and p the number of solar cells per bypass diode, then the number of diodes of bypass is given by:

$$d = \frac{c}{p} \quad (4)$$

The total voltage V_{load} must be provided for the determination of all characteristic curves. The corresponding total current, all sub-voltages and sub-currents are calculated from this total voltage. To better understand the reasoning followed, all current and voltages are shown in Fig. 5.

The total voltage is given by the expression:

$$\sum_{i=1}^c V_i - V_{load} = 0 \quad (5)$$

According to Kirchhoff's second law, the sum of the tensions in a mesh is zero:

$$\sum_{t=p \cdot (i-1)+1}^{i \cdot p} V_t + V_{c+(d-1)+i} = 0 \quad (6)$$

$$\text{for } i = 1, 2, \dots, (d-1), d$$

The currents of cells connected in series are the same for all of them:

$$I_n - I_{n+1} = 0 \quad (7)$$

for $n = (p \cdot (j-1) + 1), (p \cdot (j-1) + 1) + 1, \dots, j \cdot p - 1$
for $j = 1, \dots, d$

According to Kirchhoff's currents law, the sum of the currents in a node is zero so the ratio of the currents in the junctions where the bypass diodes are connected is:

$$I_{p,i} - I_{p,i+1} + I_{c+1} = 0, \quad \text{for } i = 1, \dots, d-1 \quad (8)$$

$$I_{c+(d-1)+i} - I_{c+1} - I_{c+(d-1)+i+1} = 0 \quad (9)$$

for $i = 1, \dots, d-1$

The total current I is obtained from the expression:

$$I_{c+d(i+1)} + I_{c+(d-1)(i+1)} - I = 0 \quad (10)$$

For a single solar cell, the relationship between the current of the cell and the voltage is:

$$-I_i + I_{ph}(i) - I_s(i) \cdot \left(e^{\frac{q(V_i + I_i \cdot R_s^{cell}(i))}{n(i) \cdot k \cdot T(i)}} - 1 \right) \quad (11)$$

$$- \frac{V_i + I_i \cdot R_s^{cell}(i)}{R_p^{cell}(i)} = 0, \quad \text{for } i = 1, \dots, c$$

Due to the presence of bypass diodes, it was not necessary to include the term related to the breakdown current of the diode as predicted in the model in which this algorithm was based. This current occurs during the avalanche effect at high negative voltages.

The equations for the diode diodes can be expressed as:

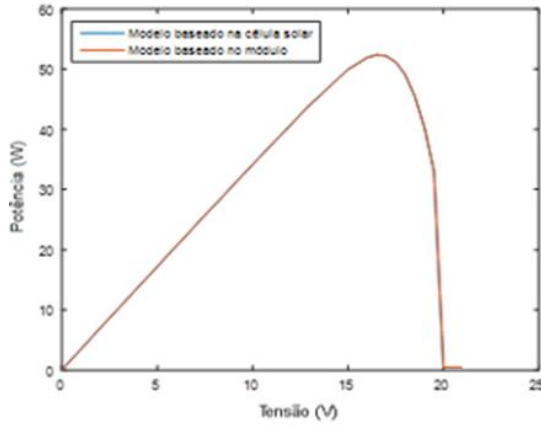
$$-I_{c+(d-1)+i} + I_{sbd} \cdot \left(e^{\frac{q(V_{c+(d-1)+1})}{n_{bd} \cdot k \cdot T_{bd}}} - 1 \right) = 0 \quad (12)$$

for $i = 1, \dots, d$

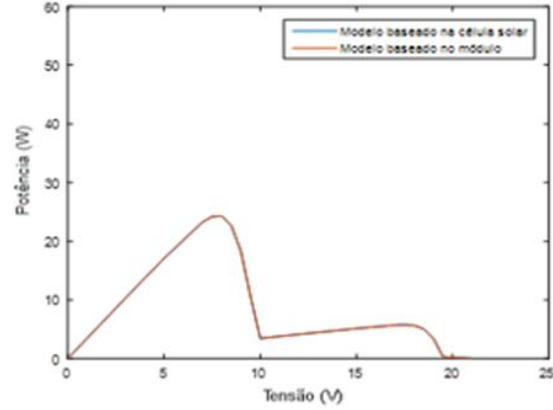
Where I_{sbd} is the saturation current of the bypass diode (1.6×10^{-9}), n_{bd} is the ideality factor (1) and T_{bd} the temperature (35°C).

The photovoltaic module Siemens SM 55 PV consists of 36 solar cells, each set of 18 cells being connected to a bypass diode. Therefore, there are a total of 78 equations and 78 unknowns. This set of equations will be solved by the method of the dogleg confidence region. [16][17]

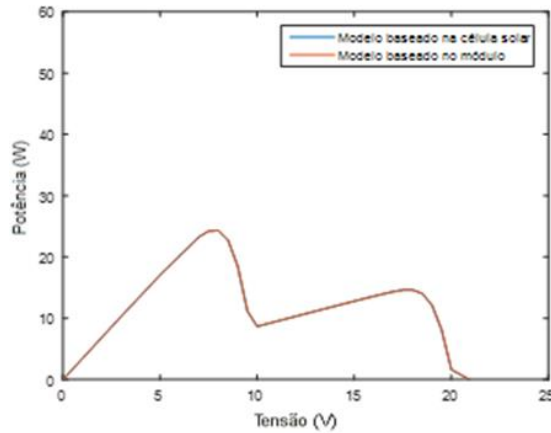
The initial values for this resolution were defined as $V_{load}/36$ for the sub-voltages and zero for the sub-currents. The equivalent circuit parameters for each solar cell are obtained



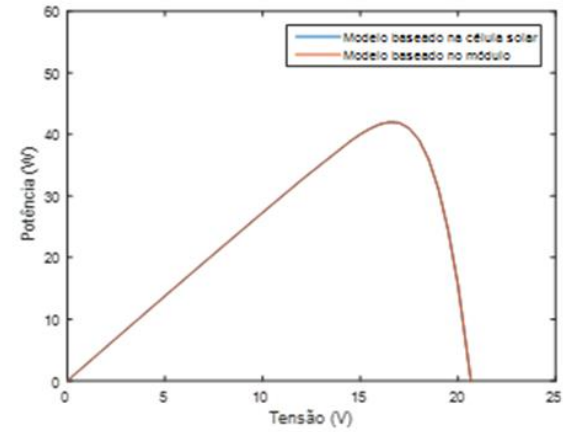
a - Sem discrepância de irradiância ($G=1000W/m^2$, $T=35^\circ C$)



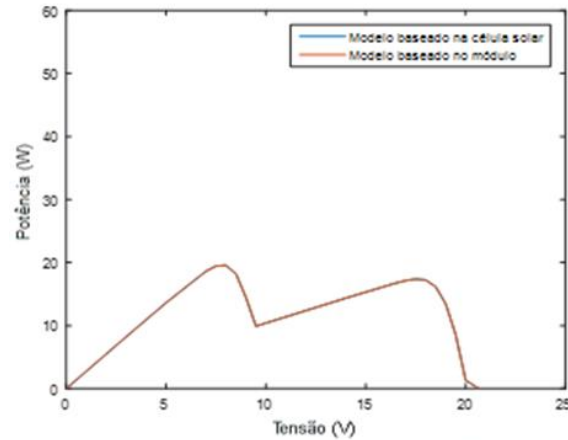
b - Para o modelo baseado na célula solar: da 1ª célula à 18ª: $100W/m^2$; para o modelo baseado no módulo: Parte-1: $100W/m^2$



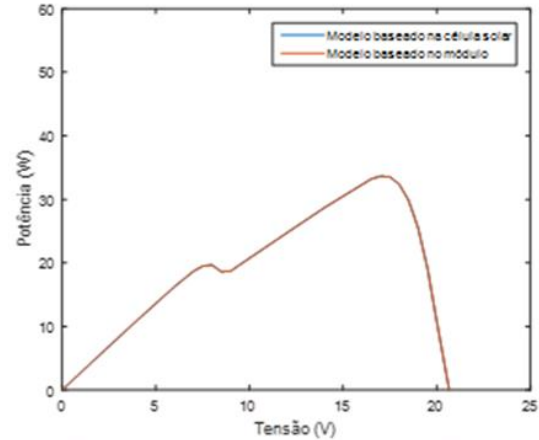
c - Para o modelo baseado na célula solar: da 1ª célula à 18ª: $250W/m^2$; para o modelo baseado no módulo: Parte-1: $250W/m^2$



d - Sem discrepância de irradiância ($G=800W/m^2$, $T=35^\circ C$)



e - Para o modelo baseado na célula solar: 1ª célula: $300W/m^2$ e 19ª célula: $800W/m^2$; para o modelo baseado no módulo: Parte-1: $300W/m^2$ e Parte-2: $800W/m^2$



f - Para o modelo baseado na célula solar: 1ª célula: $600W/m^2$ e 19ª célula: $800W/m^2$; para o modelo baseado no módulo: Parte-1: $600W/m^2$ e Parte-2: $800W/m^2$

Figure 6 - Characteristics Power-Voltage P-V for different shading conditions.

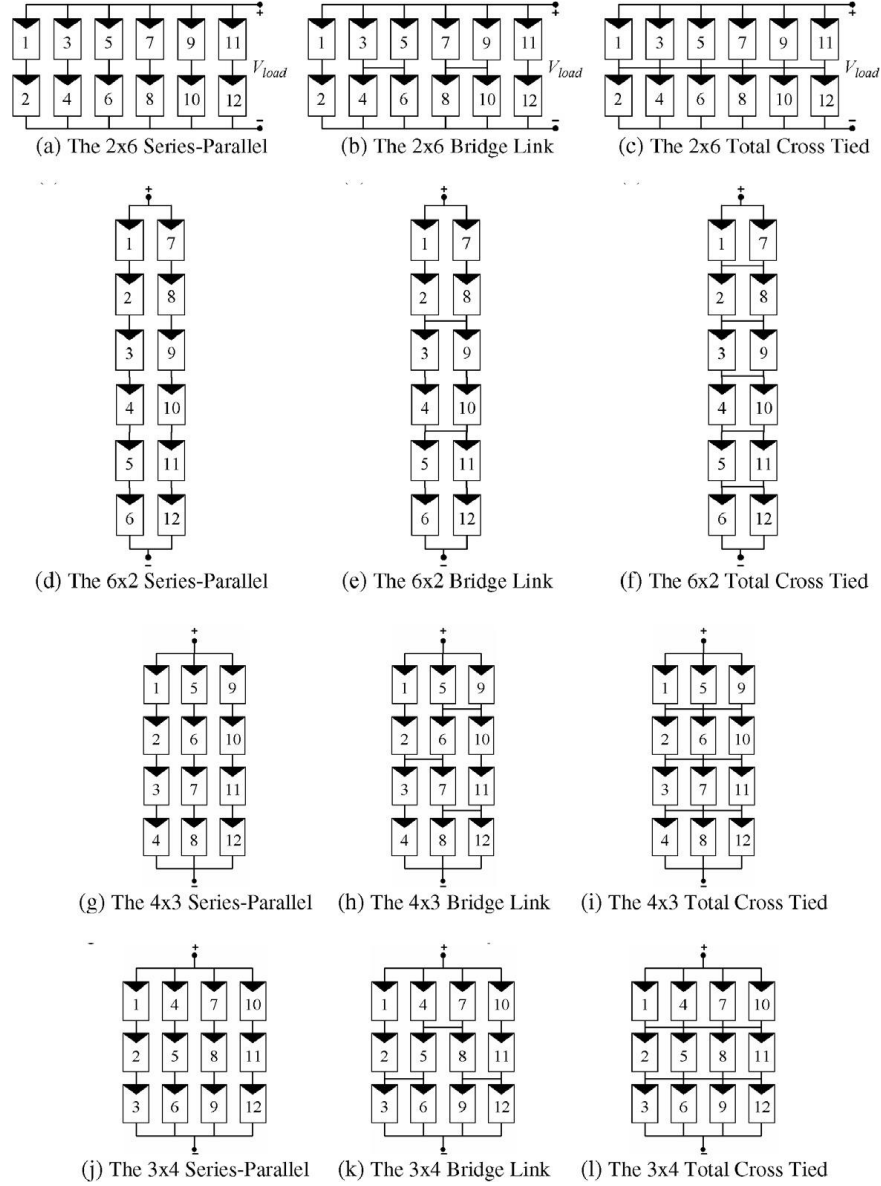


Figure 7 - Configurations of the PV array.

using ANN for each operating condition. As the ANN is trained for a single module, only the resistors R_s and R_p need to be divided by 36 for a single solar cell.

B. Module Based Method

To reduce the computational time that the cell-based method implies, the photovoltaic module is modeled in a simplified way as two modules consisting of 18 cells.

In this second algorithm the photovoltaic module is divided into two parts and each part behaves as an isolated module. The resistors R_s and R_p of each part become half of the value determined by ANN.

According to this algorithm, the I-V equation of the photovoltaic module and the deviation diode are combined in a

single equation. The equations for this model become:

$$-I_1 + I_{ph}(i) - I_s(i) \cdot \left(e^{\frac{q(V_1 + I_1 R_s(i))}{18n(i)kT(i)}} - 1 \right) \quad (13)$$

$$- \frac{V_1 + I_1 \cdot R_s(i)}{R_{p(s)}} + I_{sbd} \cdot \left(e^{-\frac{qV_1}{n_{db}kT_{bd}}} - 1 \right) = 0$$

$$V_1 + V_2 - V_{load} = 0 \quad (14)$$

$$I_1 - I_2 = 0 \quad (15)$$

For $i = 1, 2$ and where indices 1 and 2 represent Part-1 and Part-2, respectively.

In this case there are only four unknowns to obtain the I-V

characteristic of a single module.

The two algorithms are compared for different irradiance conditions and constant temperature of 35°C, and the results are shown in Fig. 6. The difference in the results obtained by the two methods is very small and it is not possible to observe them in the characteristic curves due to their reduced dimension.

IV. CURRENT-VOLTAGE CHARACTERISTICS OF PV ARRAYS

To simulate the behavior of partially shaded photovoltaic systems, for various configurations and shadowing conditions, the model based on the module previously demonstrated is used.

The 12 configurations to be tested are shown in Fig. 7. They all contain 12 Siemens SM 55 modules.

This new analysis is performed with a new algorithm, which only needs to know which configuration to examine and the size of the system. The expressions that compose the new algorithm are based on Kirchhoff's laws, in these the s represents the number of modules in a column, and r is the number of modules in a row of the PV array. To simplify the understanding of the algorithm, a general model of the photovoltaic system is described in Fig. 8, with indication of the voltages and currents.

The load voltage of the V_{load} is:

$$\sum_{i=1}^{2s} V_i - V_{load} = 0 \quad (16)$$

The Part-1 and Part-2 currents of each module must be equal:

$$I_{(j-1)2s+i} - I_{(j-1)2s+i+1} = 0 \quad \text{for } i = 1,3,5, \dots, 2s-1 \quad (17)$$

$$\text{and } j = 1,2,3, \dots, r$$

The sum of the currents at each node is zero:

$$I_{(j-1)2s+i} + I_{2sr+(j-1)(s-1)+\frac{i}{2}} - I_{(j-1)2s+i+1} \quad (18)$$

$$- I_{2sr+(j-1)(s-1)+\frac{i}{2}-(s-1)} = 0$$

for $i = 2,4,6, \dots, 2s-2$ and $j = 1,2,3, \dots, r$

with $I_{2sr+(j-1)(s-1)+\frac{i}{2}-(s-1)} = 0$ if $j=1$ and

$I_{2sr+(j-1)(s-1)+\frac{i}{2}} = 0$ if $j=r$.

The sum of the voltages in a mesh is zero:

$$V_{(j-1)2s+i-1} + V_{(j-1)2s+i} - V_{j2s+i-1} - V_{j2s+i} \quad (19)$$

$$+ V_{2sr+(j-1)(s-1)+\frac{i}{2}} - V_{2sr+(j-1)(s-1)+\frac{i}{2}-1} = 0$$

$$\text{for } i = 2,4,6, \dots, 2s \text{ and } j = 1,2,3, \dots, r-1$$

with $V_{2sr+(j-1)(s-1)+\frac{i}{2}-1} = 0$ if $i=2$ and $V_{2sr+(j-1)(s-1)+\frac{i}{2}} = 0$ if $i=2s$.

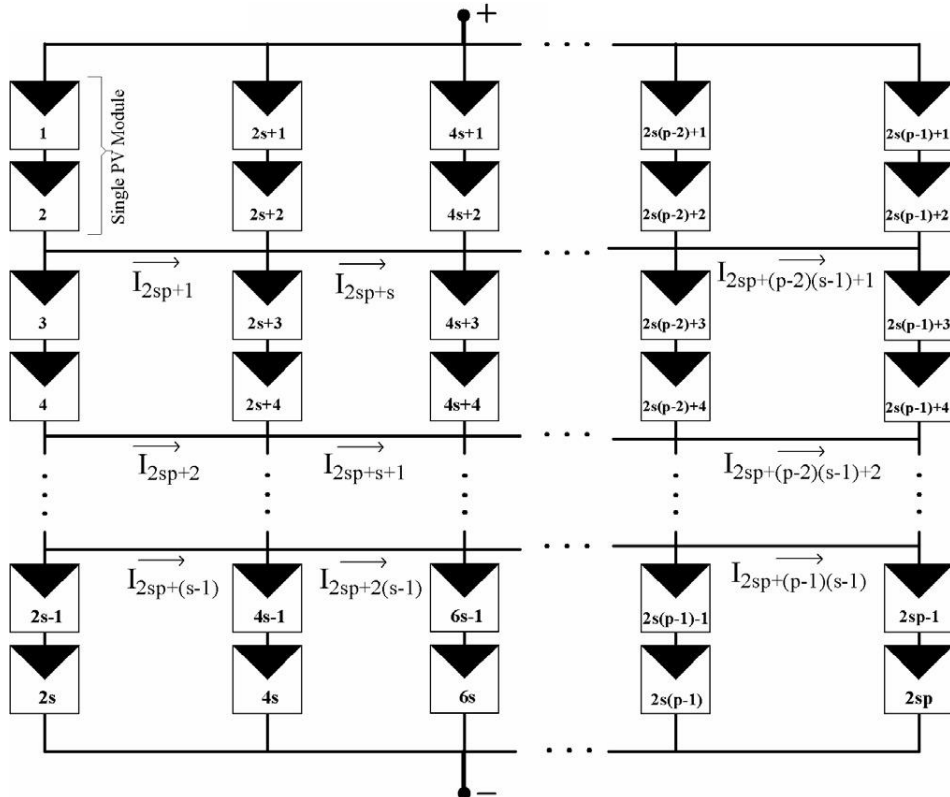


Figure 8 - General model of PV array.

For each part of the module, the relationship between current and voltage is given by the following equation:

$$-I_i + I_{ph}(i) - I_s(i) \cdot \left(e^{\frac{q(V_i + I_i R_s(i))}{18.3n(i)kT(i)}} - 1 \right) - \frac{V_i + I_i R_s(i)}{R_p(i)} + I_{sbd} \cdot \left(e^{-\frac{qV_i}{n_{db}kT_{bd}}} - 1 \right) = 0$$

for $i = 1, 2, 3, \dots, 2sr$

(20)

If the connection is serial-parallel (SP):

$$I_{2sr+(j-1)(s-1)+i} = 0 \quad \text{for } i = 1, 2, 3, \dots, s-1 \text{ and } j = 1, 2, 3, \dots, r-1$$
(21)

If the connection is total cross tied (TCT):

$$V_{2sr+(j-1)(s-1)+i} = 0 \quad \text{for } i = 1, 2, 3, \dots, s-1 \text{ and } j = 1, 2, 3, \dots, r-1$$
(22)

If the connection is bridge-linked (BL):

$$I_{2sr+(j-1)(s-1)+i} = 0 \quad \text{for } i = 1, 3, 5, \dots, s-1 \text{ and } j = 1, 3, 5, \dots, r-1$$
(23)

$$V_{2sr+(j-1)(s-1)+i} = 0 \quad \text{for } i = 1, 3, 5, \dots, s-1 \text{ and } j = 2, 4, 6, \dots, r-1$$
(24)

$$V_{2sr+(j-1)(s-1)+i} = 0 \quad \text{for } i = 2, 4, 6, \dots, s-1 \text{ and } j = 2, 4, 6, \dots, r-1$$
(25)

$$I_{2sr+(j-1)(s-1)+i} = 0 \quad \text{for } i = 2, 4, 6, \dots, s-1 \text{ and } j = 1, 3, 5, \dots, r-1$$
(26)

For each configuration, all sub-voltages and sub-currents are determined by the resolution of the system of equations described above, consisting of $2sr + (s-1)(r-1)$ equations, for various operating conditions.

To analyze the operation of photovoltaic systems, 15 random shading scenarios composed of 24 different irradiance values (12 cells each consisting of 2 parts) will be analyzed for a considered temperature of 45°C. The various shading scenarios are presented in Table 3. [18]

V. RESULTS AND DISCUSSION

The irradiance incident on a photovoltaic system is one of the factors that most influence its operation. It would be ideal if the same irradiance (and preferably a high irradiance) would affect the entire photovoltaic system uniformly, however, this is something that does not occur very often. Clouds, fog, dust, shadows caused by buildings or any other object are situations that cause shading in the photovoltaic system or in part of it.

Even when the installation is carried out in high places or in places where there are no elements that can cause shadowing, it cannot be completely avoided. Unable to be avoided, what can

be done is minimize their effects. For this, several connections are studied in detail to conclude the configuration whose shading effects are less evident.

This study was carried out considering a cell-based model, meaning that, the operation of the system was analyzed cell by cell. Therefore, the development was divided into several phases (starting from the cell to the system).

The first phase consisted in calculating the parameters of the model of a diode and five parameters of the solar cell. To do so, it was necessary to determine five points of the I-V characteristic curve of the cell for various operating conditions and, from these points, the parameters were calculated.

Due to the high computational effort required by this method, an ANN was developed based on the data obtained by the previous method. The neural network can predict the values of the five parameters of the model only based on the values of irradiance and temperature. The parameters calculated using the method based on the curve points and from the ANN are given in Table 2.

The values obtained for the parameters agree with other models that predict the variation of the parameters with the irradiance and the temperature. [10][11][12][13][14]

Then, the operation of a photovoltaic module was simulated based on the previously obtained parameters. Based on Kirchhoff's laws, a system of equations was developed which, after the resolution, provides the values of the currents and output voltages of the module to the desired irradiance values. From these, the P-V curve was obtained for the various operating conditions (Fig. 6). The cell minimally irradiated is the one that will cause most variations at P-V characteristics of the module. As shown in Fig. 6, it is irrelevant which cell is shaded, what matters is the level of irradiance.

Through these results, we can also conclude that we can consider each group of series cells as a whole module. That means that the module can be seen as two sets, each one with a bypass diode, and the results obtained will be the same.

Finally, the simulation of a photovoltaic system consisting of 12 PV modules was carried out. This simulation was performed for 12 different configurations of the system, in order to see which one minimizes the effects of non-uniform shading. For this, the different configurations were tested for various shading scenarios with random irradiance values.

After obtaining the MPPs (V_{MP} , I_{MP} and P_{MP}), the value of the maximum power when all the modules were at 1000W/m², was compared to the maximum power value for the conditions tested, and it was found the mean percentage change for each configuration, these results are shown in Table 4.

When analyzing the obtained results, it is possible to conclude that the configurations with smaller differences are those that have smaller number of modules in series. This happens because, when connected in series, the current imposed is that of the module with the lowest current, that is, the module with the lowest level of irradiance.

Contrary to other similar studies [18], where it was concluded that the best configuration would be BL, the configuration that presented the best results in the present study was 2x6-TCT.

Table 3 - Irradiances of parts 1 and 2 for the 12 modules.

Cells		Irradiances [W/m ²] for each test scenario														
		1	2	3	4	5	6	7	8	9	10	11	12	13	14	15
1	Part 1	1000	713	489	301	499	486	700	743	562	938	929	279	200	500	700
	Part 2	1000	746	616	419	784	414	987	249	609	158	496	170	200	500	700
2	Part 1	1000	763	943	134	359	203	580	229	856	114	271	542	1000	1000	1000
	Part 2	1000	599	296	393	908	400	121	478	177	226	112	798	1000	1000	1000
3	Part 1	1000	434	144	490	169	744	458	418	281	930	591	820	1000	1000	1000
	Part 2	1000	401	365	717	937	286	345	917	234	279	435	202	1000	1000	1000
4	Part 1	1000	362	582	657	260	780	665	698	624	710	171	952	1000	1000	1000
	Part 2	1000	777	707	262	395	714	493	804	962	285	329	547	1000	1000	1000
5	Part 1	1000	564	238	282	196	607	364	156	741	181	487	735	1000	1000	1000
	Part 2	1000	426	123	192	336	315	289	188	522	464	280	421	1000	1000	1000
6	Part 1	1000	219	143	824	213	447	848	807	919	994	393	888	1000	1000	1000
	Part 2	1000	649	319	355	345	221	386	150	885	587	837	809	1000	1000	1000
7	Part 1	1000	705	717	343	632	886	454	349	489	521	370	651	1000	1000	1000
	Part 2	1000	478	934	510	706	562	580	979	508	419	580	830	1000	1000	1000
8	Part 1	1000	129	537	636	357	618	186	518	564	973	206	944	1000	1000	1000
	Part 2	1000	669	872	347	119	1000	242	530	972	528	757	810	1000	1000	1000
9	Part 1	1000	821	887	315	502	161	999	473	890	122	956	354	1000	1000	1000
	Part 2	1000	902	511	856	904	501	171	146	721	320	372	733	1000	1000	1000
10	Part 1	1000	668	865	945	366	458	273	300	588	949	901	768	1000	1000	1000
	Part 2	1000	292	852	579	130	499	220	498	110	193	420	224	1000	1000	1000
11	Part 1	1000	666	773	547	107	632	708	539	994	247	494	428	1000	1000	1000
	Part 2	1000	315	834	341	375	833	178	589	488	251	442	910	1000	1000	1000
12	Part 1	1000	951	463	460	495	416	814	151	465	137	861	693	1000	1000	1000
	Part 2	1000	776	508	160	482	346	437	772	107	336	639	763	1000	1000	1000

This difference in the results may be due to the inclusion of the effect of the bypass diodes and the variation of the parameters of the equivalent circuit, in contrast to the other study.

Table 4 – Mean value of the percentage of difference between the different configurations.

Configuration		% Média
6x2	SP	55.41104
	TCT	53.66079
	BL	54.89445
2x6	SP	52.46862
	TCT	49.51557
	BL	52.21175
3x4	SP	55.16978
	TCT	50.94793
	BL	53.81213
4x3	SP	55.86738
	TCT	53.32158
	BL	54.3457

VI. CONCLUSION

In this study were tested PV arrays using a proposed PV module model based on the solar cell. The results obtained were similar to the ones that would be obtained in an empirical test, making this a valid model for characterizing shaded PV arrays. Besides that, it was shown the importance of the bypass diode, and how its inclusion on the model is essential for the good representation of the real behavior of the modules.

Results show that, to reduce the effects of shading, the number of modules connected in series should be reduced. Also, the configuration that presented the best results is the 2x6-TCT.

REFERENCES

- [1] A. Duque e S. Hegedus, Handbook of Photovoltaic Science and Engineering, John Wiley & Sons Inc., 2003
- [2] J. Duffie e W. Beckman, Solar Engineering of Thermal Processes, New Jersey: John Wiley & Sons Inc., 2013
- [3] J. Merten e et al, "Improved Equivalent Circuit and Analytical Model for Amorphous Silicon Solar Cells and Modules," *IEEE Transactions on Electron Devices*, Vol. 45, February 1998
- [4] A. Labouret e M. Viloz, Solar Photovoltaic Energy, London: Institute of Energy and Technology, Fourth Edition, 2010
- [5] D. L. King, W. E. Boyson e J. A. Kratochvill, Photovoltaic Array Performance Model, Albuquerque, New Mexico: Sandia National Laboratories, December 2004
- [6] F. J. Toledo, J. M. Blanes e V. Galiano, "Two-Step Linear Least-Squares Method for Photovoltaic Single-Diode Model Parameters Extraction," *IEEE Transactions on Industrial Electronics*, Vol. 65, 2018
- [7] K. J. Singh, K. L. R. Koh e et al, "Artificial Neural

Network Approach for more Accurate Solar Cell Electrical Circuit Model," *International Journal on Computational Sciences & Applications*, Vol. 4, June 2014

[8] F. Dkhichi e B. Oukarfi, "Determination of Solar Cell Parameters using Neural Network Trained by Steepest Descent Algorithm," *International Journal of Advanced Research in Computer Science and Software Engineering*, Vol. 4, August 2014

[9] A. Gastli e M. Rhouma, "ANN - Based Extraction Approach of PV Cell Equivalent Circuit Parameters," *Conference paper for the 17th European Conference on Power Electronics and Applications*, Switzerland, September 2015

[10] M. A. Blas, J. L. Torres, E. Prieto e A. Garcia, "Selecting a Suitable Model for Characterizing Photovoltaic Devices," *Renewable Energy*, Vol. 25, 2002

[11] A. K. Sharma, R. Dwivedi e S. K. Srivastava, "Performance Analysis of a Solar Array Under Shadow Condition," *IEEE Proceedings*, 1991

[12] A. Virtuani, E. Lotter e M. Powalla, "Performance of Cu(In,Ga)Se₂ Solar Cells Under Low Irradiance," *Thin Solid Films*, 2003

[13] J. Ding, X. Cheng e T. Fu, "Analysis of Series Resistance and P-T Characteristics of the Solar Cell," *Vacuum*, Vol. 77, 2005

[14] N. Veissid e A. M. de Andrade, "The I-V Silicon Solar Cell Characteristic Parameters Temperature Dependence. An Experimental Study using the Standard Deviation Method," em *Proceedings of the 10th European Photovoltaic Solar Energy Conference*, Lisboa, Portugal, 1991

[15] V. Quaschnig e R. Hanitsch, "Numerical Simulation of Current-Voltage Characteristics of Photovoltaic Systems with Shaded Solar Cells," *Solar Energy*, Vol. 56, 1996

[16] M. J. D. Powell, "A Fortran Subroutine for Solving Systems of Nonlinear Algebraic Equations," *Numerical Methods for Nonlinear Algebraic Equations*, p. Ch. 7, 1970

[17] J. E. Dennis Jr. e R. B. Schnabel, Numerical Methods for Unconstrained Optimization and Nonlinear Equations, Philadelphia: Society for Industrial and Applied Mathematics, 1996.

[18] N. D. Kaushika e N. K. Gantam, "Energy Yield Simulation of Interconnected Solar PV Arrays," *IEEE Transactions on Energy Conversion*, Vol 18, March 2003.